Computational scheme for *ab-initio* predictions of chemical compositions interfaces realized by deposition growth

Jochen Rohrer and Per Hyldgaard

BioNano Systems Laboratory, Department of Microtechnology, MC2, Chalmers University of Technology, SE-412 96 Gothenburg

Abstract

We present a novel computational scheme to predict chemical compositions at interfaces as they emerge in a growth process. The scheme uses the Gibbs free energy of reaction associated with the formation of interfaces with a specific composition as predictor for their prevalence. It explicitly accounts for the growth conditions by rate-equation modeling of the deposition environment. We illustrate the scheme for characterizing the interface between TiC and alumina.

Keywords: DFT, chemical vapor deposition, CVD, growth, atomistic modeling

1. Introduction

Density functional theory calculations are today routinely applied to characterize structural and electronic properties of condensed matter systems. They serve as an important complement to and extension of experimental methods [1]. Atomic (and electronic) structure and chemical composition are inseparably interwoven. Information about chemical composition at, for example, interfaces (including surfaces) is therefore of great importance for reliability of such calculations.

Traditional *ab initio* atomistic thermodynamics methods aim at describing and predicting compositions at oxide surfaces [2, 3]. These schemes assume that equilibrium is established between the oxide and surrounding O_2. This criterion is often justified for oxide surfaces that are in direct contact with an O-rich environment. For (solid-solid) interfaces, the situation is more complicated. Interfaces are typically exposed to the surrounding environment only at the moment of creation.[1] Furthermore, oxides are seldomly grown directly from O_2, and it is not clear what gas(es) they are in (dynamic) equilibrium with during deposition, if at all. A generalization of the *ab initio* atomistic thermodynamics scheme from surfaces to interfaces [4] can therefore be problematic. In fact, we have shown [5] that the equilibrium configuration at the interface between TiC and alumina predicted by such a generalized scheme does not describe the wear-resistance of TiC/alumina multilayer coatings [6]. We have attributed this inconsistency to the fact that the scheme does not account for the actual growth conditions. This may be a serious shortcoming also for other interfaces realized by deposition growth.

This paper presents a computational scheme that explicitly accounts for deposition conditions. At the same time no *a priori* equilibrium assumptions are introduced. The scheme is therefore capable to predict chemical compositions at interfaces (including surfaces) as they arise in a deposition process. The key elements of this scheme are the use of Gibbs free energies of reaction as a predictor for the chemical composition and a modeling of the deposition conditions in terms of rate equations describing deposition environment. The approach extends the method of *ab initio* thermodynamics of deposition growth for surfaces [7] to interface modeling.

The paper is organized as follows. Section 2 motivates the use of the Gibbs free energy of reaction as a predictor of chemical composition. Section 3 contains the details of our modeling. Results are presented in Sec. 4 and Sec. 5 contains our conclusions.

2. Predictor for as-grown chemical composition

We use the Gibbs free energies of reaction G_r as a predictor for the prevalent chemical composition at surfaces and interfaces realized by deposition growth. We justify the use of G_r as predictor using chemical reaction theory [8, 9].

The Gibbs free energy of reaction is defined as the gain in Gibbs free energy in a chemical reaction. For a general reaction, according to chemical reaction theory, G_r is related to the forward (f) and backward (b) reaction rates $\Gamma_f = k_f \Pi_r [\mathrm{R}_r]^{\nu_r}$ and $\Gamma_b = k_b \Pi_p [\mathrm{P}_p]^{\nu_p}$ via

$$-\beta G_r = \ln \Gamma_f / \Gamma_b \tag{1}$$

Here β is the inverse temperature in units of energy, $k_{\{f,b\}}$ is forward and backward rate constant, $[\mathrm{R}_r]$ ($[\mathrm{P}_p]$) is the concentration of the r-th (p-th) reactant R (product P), and $\nu_{\{p,r\}}$ is the corresponding stoichiometric coefficient.[2]

[1] In this study we assume that the interface is created by a deposition process from a gas phase.

[2] In this section we count stoichiometric coefficients positively, opposed to standard chemical nomenclature, where stoichiometric coefficients of reactants are counted negatively.

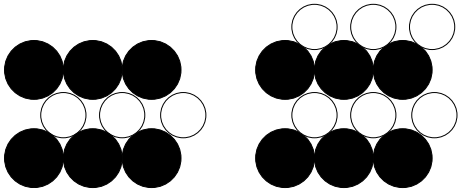

Figure 1: Illustration of two different terminations at the surface of a binary material AB.

To illustrate the approach, we first discuss the problem of surface termination in deposition growth [7], seeking to predict which surface (A terminated or B terminated) will emerge when growing a binary material AB, see Fig. 1. We consider two coupled reactions I and II that change the surface termination from A to B and vice versa,

$$I: \ \mathrm{B} + \mathrm{React}_I \underset{\Gamma_b^I}{\overset{\Gamma_f^I}{\rightleftharpoons}} \mathrm{A} + \mathrm{Prod}_I \tag{2a}$$

$$II: \ \mathrm{A} + \mathrm{React}_{II} \underset{\Gamma_b^{II}}{\overset{\Gamma_f^{II}}{\rightleftharpoons}} \mathrm{B} + \mathrm{Prod}_{II}. \tag{2b}$$

Here, $\mathrm{React}_{\{I,II\}}$ and $\mathrm{Prod}_{\{I,II\}}$ collectively denote the reactants and products in the two reactions. The forward and backward rates are the same as in (1) but have an additional index to differentiate between the two reactions. Taking the difference between the free energies of reaction in I and II, we find after exponentiation and use of the geometric mean $\langle x,y\rangle_{\mathrm{gm}} = (xy)^{-1/2}$

$$\exp\left(-\beta[G_r^I - G_r^{II}]\right) = \frac{\Gamma_f^I\Gamma_b^{II}}{\Gamma_b^I\Gamma_f^{II}} = \left[\frac{\langle\Gamma_f^I,\Gamma_b^{II}\rangle_{\mathrm{gm}}}{\langle\Gamma_b^I,\Gamma_f^{II}\rangle_{\mathrm{gm}}}\right]^2. \tag{3}$$

The reactions in (2) can also by described by the rate equations,

$$\partial_t P_{\mathrm{A}} = -(\Gamma_b^I + \Gamma_f^{II})P_{\mathrm{A}} + (\Gamma_f^I + \Gamma_b^{II})P_{\mathrm{B}} \tag{4a}$$

$$\partial_t P_{\mathrm{B}} = (\Gamma_b^I + \Gamma_f^{II})P_{\mathrm{A}} - (\Gamma_f^I + \Gamma_b^{II})P_{\mathrm{B}}. \tag{4b}$$

Here we have introduced the probability $P_{\{\mathrm{A,B}\}}$ for observing either an A or B terminated surface. Using the arithmetic mean $\langle x,y\rangle_{\mathrm{am}} = (x+y)/2$, the steady-state solution provides a ratio between these probabilities,

$$\frac{P_{\mathrm{A}}}{P_{\mathrm{B}}} = \frac{(\Gamma_f^I + \Gamma_b^{II})}{(\Gamma_b^I + \Gamma_f^{II})} = \frac{\langle\Gamma_f^I,\Gamma_b^{II}\rangle_{\mathrm{am}}}{\langle\Gamma_b^I,\Gamma_f^{II}\rangle_{\mathrm{am}}}. \tag{5}$$

In dynamic equilibrium [8, 9], being characterized by $G_r^I + G_r^{II} = 0$ or equivalently $\Gamma_f^I/\Gamma_b^{II} = \Gamma_b^I/\Gamma_f^{II}$, we find by combining (3) and (5) that

$$\frac{P_{\mathrm{A}}}{P_{\mathrm{B}}}\Big|_{\mathrm{dyn.\ eq.}} = \exp\left(-\beta[G_r^I - G_r^{II}]/2\right). \tag{6}$$

In particular, if the reaction that creates an A-terminated surface has lower G_r than the reaction that creates a B-terminated surface, here $G_r^I < G_r^{II}$, an A-terminated surface is more likely. Away from dynamic equilibrium, this relation is no longer exact. However, our comparison of G_r for different terminations still indicates which termination is most prevalent, since the geometric and arithmetic means [Eqs. (3) and (5)] are approximately equal, Ref. [7].

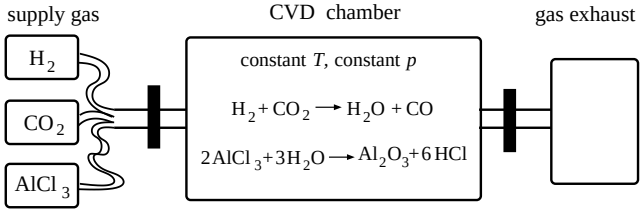

Figure 2: Illustration of chemical vapor deposition of alumina. A H_2-$AlCl_3$-CO_2 gas mixture is supplied to a chamber at rate R_S. The chamber is kept at fixed temperature T and fixed total pressure p. The gases react to simultaneously form water and alumina. Reaction products and unused reactants are exhausted at rate R_E.

By analogy to the case of surface terminations, we use G_r as measure to predict chemical compositions at interfaces formed by deposition growth (and assumed to have retained the structure specified by the deposition environment). Considering related interface configurations of similar thickness but different compositions, the one with lowest (most negative) Gibbs free energy of reaction is most likely to describe the nature of the interface as it is formed by deposition growth. We note that G_r will in general decrease (if the reaction is favorable) as the number of constituents in the film describing the interface increases by any integer multiple of the bulk stoichiometry. Our predictor is useful when comparing films of similar thickness.

3. Modeling

3.1. Materials Background

We illustrate our computational scheme by studying the interface composition between TiC and alumina. TiC/alumina multilayers are commonly used as wear-resistant coating on cemented-carbide cutting tools [6]. They are routinely fabricated by chemical vapor deposition (CVD).

Figure 2 illustrates the experimental setup for CVD of alumina [10]. A H_2-$AlCl_3$-CO_2 supply gas mixture is injected into a hot chamber which is kept at a fixed temperature and a fixed total pressure. The CVD process proceeds in two steps which, however, take place in parallel. Water forms at an (unknown) rate $R_{\mathrm{H_2O}}$ according to

$$\mathrm{H_2} + \mathrm{CO_2} \xrightarrow{R_{\mathrm{H_2O}}} \mathrm{H_2O} + \mathrm{CO}. \tag{7}$$

Alumina is deposited at an (unknown) rate $R_{\mathrm{Al_2O_3}}$ according to

$$2\mathrm{AlCl_3} + 3\mathrm{H_2O} \xrightarrow{R_{\mathrm{Al_2O_3}}} \mathrm{Al_2O_3} + 6\mathrm{HCl}. \tag{8}$$

3.2. Ab initio structure search for thin alumina films and TiC/alumina interface models

In Refs. [5, 11, 12] we have (in collaboration with others) presented a computational strategy for identifying energetically favorable geometries of thin-film alumina on a TiC substrate.

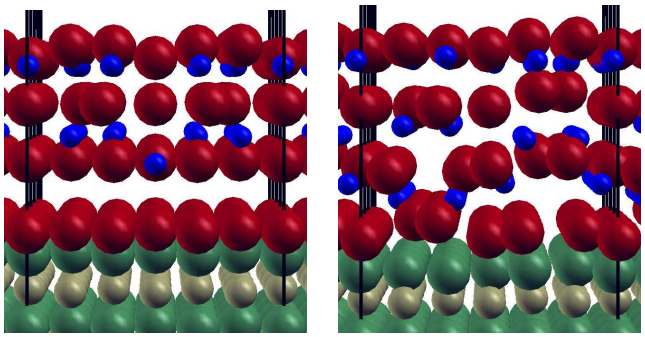

Figure 3: Exfoliating (left panel) and wear-resistant alumina (right panel) films on TiC. Color coding: Ti = dark green, C = light green, Al = blue, O = red.

We have constructed alumina candidate configurations from a pool of structural motifs as they exist in stable and metastable bulk alumina phases. The motifs are characterized by stacking of the O layers and by the coordination of the Al ions. We have considered alumina films of thicknesses up to four O layers. In addition, we allowed for off-stoichiometric compositions of these films.

Each candidate configuration was structurally optimized by *ab initio* total-energy and force calculations and subsequent relaxation (using standard quasi-Newton and conjugate gradient algorithms). For a given thickness and stoichiometric composition, the optimal geometry was identified as the one with lowest total energy after structural relaxations.

Figure 3 details the atomic structure of two optimized alumina films with a thickness of four O layers and different stoichiometric compositions. These films are referred to as exfoliating (left) and wear-resistant (right) films. These terms describe the nature of adhesion properties in the two films (exfoliating = no or very weak adhesion, wear-resistant = strong adhesion). Details concerning adhesion properties of these films will be given elsewhere [13]. For other thicknesses, the films possess similar structural (and adhesion) characteristics. Focusing on the films explicitly shown in Fig. 3 does not imply a restriction of generality in our present discussion of the TiC/alumina interface.

The results of our (total-energy) structure search (for each class of Al_MO_N films) can be combined with the equilibrium thermodynamics of Refs. [2, 3, 4]). We find that this approach erroneously identifies the exfoliating film as thermodynamically stable [5]. This incrorrect prediction results from the old equilibrium theory accross a wide range of temperatures and O_2 pressures and the theory is in conflict with wear-resistance of TiC/alumina multilayer coatings [6]. Below we show that a more physical account of alumina growth emerges with our new nonequilibrium thermodynamics theory.

3.3. Formation of excess atoms and free energies of reaction

The films shown in Fig. 3 can be divided into a stoichiometric part and an excess part. For a general Al_MO_N film, the number of stoichiometric units in the stoichiometric part of the film is $n_{\text{alumina}} = \min([M/2],[N/3])$, where $[x]$ is the largest integer smaller or equal to x. The corresponding number of excess Al and O atoms is $\Delta n_{\text{Al}} = N - 2n_{\text{alumina}}$ and $\Delta n_{\text{O}} = M - 3n_{\text{alumina}}$.

We assume that the deposition of the stoichiometric parts of the films is described by (8). Excess O can be deposited as

$$\text{CO}_2 \rightarrow \text{O}_{\text{exc}} + \text{CO}, \tag{9a}$$

$$\text{H}_2\text{O} \rightarrow \text{O}_{\text{exc}} + \text{H}_2, \tag{9b}$$

depending on which reaction gives a lower free energy of reaction. (Excess Al is not considered here.) The free energy of reaction is defined accordingly,

$$G_{\text{r}}^{\text{Al}_M\text{O}_N} = G_{\text{TiC/Al}_M\text{O}_N} - G_{\text{TiC}} + n_{\text{Al}_2\text{O}_3}\left(6\mu_{\text{HCl}} - 2\mu_{\text{AlCl}_3} - 3\mu_{\text{H}_2\text{O}}\right) + \Delta n_{\text{O}} \max\left[\mu_{\text{CO}} - \mu_{\text{CO}_2}, \mu_{\text{H}_2} - \mu_{\text{H}_2\text{O}}\right]. \tag{10}$$

3.4. Approximations for evaluation of G_r

We make standard approximations for the free energy of solid and gaseous constituents. The free energy of the TiC/alumina systems is approximated by their DFT total energies, that is, $G_{\text{solid}} \approx E_{\text{solid}}$.[3] Vibrational effects are not considered [3, 7]. For gaseous constituents, we employ the ideal-gas approximation,

$$\mu_i(T, p_i) = \epsilon_i + \Delta_i^0(T) + k_B T \ln(p_i/p^0). \tag{11}$$

Here ϵ_i is the DFT total energy [14] of the gas phase species (molecule), and k_B is the Boltzmann constant. $\Delta_i^0(T)$ is the temperature dependence of μ_i at a fixed pressure p^0, and available for $p^0 = 1$ atm in thermochemical tables [15].

3.5. Rate-equation description of CVD of alumina

The evaluation of the individual chemical potentials of the different gaseous constituents in the CVD chamber requires the specification of the associated partial pressures. In the actual fabrication process, these are, however, not directly controlled; only the temperature and the total pressure are controlable.

We describe the CVD process in terms of rate equations for the individual (ideal gas) pressures,

$$\partial_t p_i \propto c_i R_{\text{S}} - \frac{p_i}{p} R_{\text{E}} + \nu_i^{\text{H}_2\text{O}} R_{\text{H}_2\text{O}} + \nu_i^{\text{Al}_2\text{O}_3} R_{\text{Al}_2\text{O}_3}. \tag{12}$$

Here, $p_i = p_i(t)$ is the pressure of chemical species i at time t inside the reaction chamber, $p = p(t) = \sum_i p_i(t)$ is the corresponding total pressure, c_i is the concentration of the chemical species i in the supply gas, and $\nu_i^{\text{H}_2\text{O}}$ and $\nu_i^{\text{Al}_2\text{O}_3}$ are the stoichiometric coefficients[4] of the the chemical species i in reaction (7) and (8), respectively The rate at which the gas is supplied to (exhausted from) the chamber is R_{S} (R_{E}) and the reaction rates for water production and alumina deposition are $R_{\text{H}_2\text{O}}$ and $R_{\text{Al}_2\text{O}_3}$.

[3] In fact, we correct the total energies of the films by subtracting the strain energy of the stoichiometric part of the film, $E_{\text{film}} \rightarrow E_{\text{film}} - n_{\text{Al}_2\text{O}_3}\Delta_{\text{strain}}$, where Δ_{strain} is the is difference between the strained (due to the expansion to the TiC lattice in the interface plane) and the unstrained bulk alumina per stoichiometric unit.

[4] Here we use the standard conventions that stoichiometric coefficients are counted negative if a species is consumed and positive if a species is produced in a reaction.

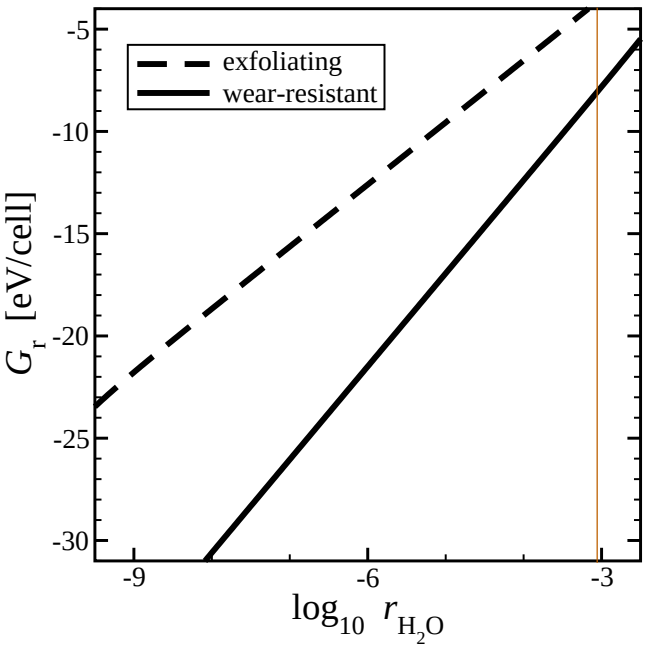

Figure 4: Gibbs free energies of reaction G_r for exfoliating and wear-resistant alumina film (see Fig. 3) as functions of the scaled reaction rate r_{H_2O}. The vertical line limits r_{H_2O} to the right and corresponds to dynamic equilibrium in (7). For simplicity, we assume $R_{Al_2O_3} = R_{H_2O}/3$.

We use the resulting steady-state pressures

$$p_i = p\frac{c_i + r_{H_2O}\nu_i^{H_2O} + r_{Al_2O_3}\nu_i^{Al_2O_3}}{1 + r_{Al_2O_3}}, \qquad (13)$$

as input for the evaluation of the individual chemical potentials (11). In (13) we have introduced the scaled reaction rates $r_{H_2O} = R_{H_2O}/R_S$ and $r_{Al_2O_3} = R_{Al_2O_3}/R_S$.

3.6. Limits on reaction rates

The reaction rates R_{H_2O} and $R_{Al_2O_3}$ cannot assume any arbitrary value. For example, we require that $R_{Al_2O_3} \leq R_{H_2O}/3 = R^{max}_{Al_2O_3}$, since reaction (8) requires three units of H_2O, while reaction (7) produces only one. Additional constraints on this particular growth process and interface formation will be discussed in a forthcoming publication [13].

4. Results

In Fig. 4 we plot the free energies of reaction for the two films shown in Fig. 3 as functions of the scaled reaction rate r_{H_2O}. Deposition parameters (supply gas composition, total pressure, and deposition temperature) as specified in Ref. [10] have been used. In this illustration of the approach we assume for simplicity $R_{Al_2O_3} = R_{H_2O}/3$. Furthermore, the scaled reaction rate r_{H_2O} is limited to the right by the limit of dynamic equilibrium in (7), indicated by the vertical line.

We find that, over the entire range of the reaction rate r_{H_2O}, it is more favorable to grow wear-resistant overlayers than exfoliating overlayers.[5] This qualitative result is independent of the choice of $R_{Al_2O_3}$, and (unlike for the analysis based on equilibrium thermodynamics [5]) it is consistent with industrial usage of TiC/alumina as wear-resistant coating.

5. Summary & Conclusions

We have presented a novel computational scheme to predict chemical compositions at interfaces as they emerge in a growth process. The scheme uses the Gibbs free energy of reaction associated with the formation of interfaces with a specific composition as predictor for their prevalence. We explicitly account for the growth conditions by rate-equation modeling of the deposition environment. An earlier study [5] documented that the composition at this interface is in conflict with the wear-resistance of multilayered TiC/alumina when using an equilibrium-thermodynamics scheme [2, 3, 4]. Our results demonstrate that a careful account of deposition conditions in interface modeling is crucial for understanding the adhesion at CVD TiC/alumina.

We expect that a similar analysis will be necessary also for other buried interfaces that form during a deposition process in an environment that strongly differs from ambient conditions. We emphasize the predictive power of the here-presented method, adding to the DFT-based toolbox for accelerating innovation [16]. In principle, it allows for the determination of deposition conditions required to experimentally create interfaces with a predetermined compositions. We argue that combining the structure search method of Ref. [5] and the new *ab initio* thermodynamics with, for example, a genetic algorithm [17, 18] presents a valuable tool for characterization of surface and interface growth.

Acknowledgments

We thank Carlo Ruberto and Gerald D. Mahan for valuable discussions. We gratefully acknowledge support from the Swedish National Graduate School in Materials Science (NFSM), from the Swedish Foundation for Strategic Research (SSF) through ATOMICS, from the Swedish Research Council (VR) and from the Swedish National Infrastructure for Computing (SNIC).

References

[1] as exemplified by G. Kresse, M. Schmid, E. Napetschnig, M. Shishkin, L. Kohler, and P. Varga, Structure of the Ultrathin Aluminum Oxide Film on NiAl(110), *Science* **308** (2005) 1440; X.G. Wang, A. Chaka, and M. Scheffler, Effect of the Environment on α-Al2O3 (0001) Surface Structures, *Phys. Rev. Lett.* **84** (2000) 3650; A. Marmier and S. C. Parker, Ab initio morphology and surface thermodynamics of -Al2O3, *Phys. Rev. B* **69** (2004) 115409.

[5] We notice that there is a third stoichiometric composition (not discussed in this work) that may be stabilized if r_{H_2O} is sufficiently far away from the dynamic equilibrium limit. The corresponding structure has also wear-resistant properties.

[2] I. G. Batyrev, A. Alavi, and M. W. Finnis, Equilibrium and adhesion of Nb/sapphire: The effect of oxygen partial pressure, *Phys. Rev. B* **62** (2000) 4698.
[3] K. Reuter and M. Scheffler, Composition, structure, and stability of RuO2(110) as a function of oxygen pressure, *Phys. Rev. B* **65** (2001) 035406.
[4] W. Zhang, J. R. Smith, and X.G. Wang, Thermodynamics from ab initio computations, *Phys. Rev. B* **70** (2004) 024103.
[5] J. Rohrer, C. Ruberto, and P. Hyldgaard, *Ab initio* structure modelling of complex thin-film oxides: thermodynamical stability of TiC/thin-film alumina, *J. Phys.: Condens. Matter* **22** (2010) 015004. See also the corresponding supplementary material, available online.
[6] M. Halvarsson, H. Norden, and S. Vuorinen, Microstructural investigation of CVD α-Al2O3/κ-Al2O3 multilayer coatings, *Surf. Coat. Technol.* **61** (1993) 177.
[7] J. Rohrer and P. Hyldgaard, *Ab initio* thermodynamics of deposition growth: Surface terminations of TiC(111) and TiN(111) grown by chemical vapor deposition, submitted to *Phys. Rev. B*; see also arXiv:1004.1929v1 [cond-mat.mtrl-sci].
[8] Y. Demirel, *Nonequilibrium Thermodynamics: Transport and Rate Processes in Physical, Chemical and Biological Systems*, 2nd ed. (Elsevier, Amsterdam, 2007).
[9] N. Tschoegl, *Fundamentals of equilibrium and steady-state thermodynamics*, 1st ed. (Elsevier, Amsterdam, 2000).
[10] S. Ruppi and A. Larsson, Chemical vapour deposition of κ-Al2O3, Thin Solid Films **388** (2001) 50.
[11] S. Canovic, S. Ruppi, J. Rohrer, A. Vojvodic, C. Ruberto, P. Hyldgaard, and M. Halvarsson, TEM and DFT investigation of CVD TiN/κ-Al2O3 multilayer coatings, *Surf. Coat. Technol.* **202** (2007) 522.
[12] J. Rohrer, A. Vojvodic, C. Ruberto, and P. Hyldgaard, Coarse-grained model for growth of α- and κ-Al2O3 on TiC and TiN(111): thin alumina films from density-functional calculations, *J. Phys.: Conf. Ser.* **100** (2008) 082010.
[13] J. Rohrer and P. Hyldgaard, unpublished.
[14] We use the DFT code Dacapo (B. Hammer, O. H. Nielsen, J. J. Mortensen, L. Bengtsson, L. B. Hansen, A. C. E. Madsen, Y. Morikawa, T. Bligaard, A. Christensen, J. Rossmeisl, available from https://wiki.fysik.dtu.dk/dacapo) for the evluation of these energies with the same energy cutoff as in Ref. [5], and Brilluoin zone sampling at the Γ point of a supercell of size 20×20×20 Å^3.
[15] M. W. Jr. Chase (Ed.), *NIST-JANAF Thermochemical Tables* (Washington, DC : American Chemical Society ; New York : American Institute of Physics for the National Institute of Standards and Technology, 1998).
[16] For example, as discussed in T. S. Rahman, Computational methodologies for designing materials, *J. Phys.: Condens. Matter* **21**, 080301 (2009). and Ø. Borck, P. Hyldgaard, and E. Schröder, Adsorption of methylamine on α-Al2O3(0001) and α-Cr2O3(0001): Density functional theory, *Phys. Rev. B* **75**, 035403 (2007).
[17] A. L.-S. Chua, N. A. Benedek, L. Chen, M. W. Finnis, and A. P. Sutton, A genetic algorithm for predicting the structures of interfaces in multicomponent systems, Nature Materials **9** (2010) 418.
[18] J. Rohrer and P. Hyldgaard, unpublished.